1D chain coordination assembly of $[Mn_4(hmp)_6(NO_3)_2]^{2+}$ single-molecule magnets linked by the photochromic $[FeNO(CN)_5]^{2-}$ precursor

Lyudmila A. Kushch [a,*], Valentina D. Sasnovskaya [a], Eduard B. Yagubskii [a,*], Salavat S. Khasanov [b], Sergey V. Simonov [b], Rimma P. Shibaeva [b], Alexander V. Korolev [c], Denis V. Starichenko [c], Anatoly O. Anokhin [c], Valentin Yu. Irkhin [c], Yuri N. Shvachko [c]

[a] Institute of Problems of Chemical Physics of Russian Academy of Science, Semenov's av., 1, Chernogolovka 142432, MD, Russia
[b] Institute of Solid State Physics of Russian Academy of Sciences, 2 Academician Ossipyan str., Chernogolovka 142432, MD, Russia
[c] Institute of Metal Physics, Ural Branch of Russian Academy of Sciences, Kovalevskaya str., 18, Ekaterinburg 620041, Russia

ARTICLE INFO

ABSTRACT

The first heterometallic chain cluster $\{[Mn_4(hmp)_6(NO_3)_2FeNO(CN)_5\cdot4CH_3CN\}_n$ (**1**) based on the $[Mn_4(hmp)_6]$ SMM has been synthesized. **1** has one-dimensional chain structure: the $[Mn_4(hmp)_6]$ units are linked via CN-groups of nitroprusside anions. Its magnetic and relaxation properties and low temperature IR spectra under light irradiation have been investigated. The ferromagnetic exchange constants have been calculated.

© 2011 Elsevier B.V. All rights reserved.

1. Introduction

In the last few years, the design and synthesis of molecular nanomagnets, so-called single-molecule magnets (SMMs) and single-chain magnets (SCMs), have became the main research trend in the field of molecular magnetism [1]. Both the class of molecular nanomagnets have attracted widespread attention owing to their unusual properties to scale a single molecule or a single polymeric chain (superparamagnetism, slow magnetic relaxation, magnetic hysteresis, blocking and quantum tunneling of the magnetization, and quantum interference) [2]. These nano-scale magnetic materials are of great interest for both fundamental science and practical applications such as high-density information storage, quantum computers, spin transistors, and molecular spintronics [3]. Most SMMs are magnetic clusters of transition-metal ions surrounded by shells of ligand molecules. Their unique magnetic properties result from combination of a large total spin ground state and a strong uniaxial magnetic anisotropy which give rises to a barrier to magnetic relaxation. SCMs are essentially one-dimensional analogs of SMMs. Many of them are built from the anisotropic magnetic blocks

(SMMs) which are linked by bridging ligands in the chains with strong intrachain magnetic interactions, and negligible interchain interactions [2d–2h]. Compared to other type magnetic nanoparticles, the molecular nanomagnets have important advantages: they are uniform and their structure and magnetic properties can be tuned by coordination chemistry methods; furthermore, the interesting combinations of their magnetic properties with other properties (optical, conducting) are possible [4]. Photochromic SMMs based on anion oxocarboxylate clusters of Mn12 with photochromic mononitrosyl complexes of Ru as counter ions were synthesized [5]. The reversible photoswitching magnetic system involving 1D chain coordination assemblies of $[Mn_4(hmp)_6]$ SMMs (hmp = 2-hydroxymethylpyridine) linked by the photochromic diarylethene ligands has been recently found [6]. The bimetallic cyanido-bridged magnetic material $[\{Mn_2(saltmen)_2\}_2FeNO(CN)_5](ClO_4)_2\cdot2CH_3CN\cdotH_2O$ (saltmen^{2-} = N,N'- (1,1,2,2-tetramethylethylene)bis(salicylideneiminato) dianion) derived from dinuclear cluster $[\{Mn(saltmen)\}_2]^{2-}$ and photochromic pentacyanidonitrosylferrate(II) precursor (nitroprusside anion) was prepared [7].

We studied the reaction of the cationic SMM $[Mn_4(hmp)_6$ $(NO_3)_2(H_2O)_2]^{2+}(ClO_4)_2\cdot4H_2O$ [8], with nitroprusside anion in CH_3CN and synthesized the first bimetallic chain cluster $\{[Mn_4(hmp)_6$ $(NO_3)_2FeNO(CN)_5\cdot4CH_3CN\}_n$ (**1**) based on the $[Mn^{II}_2Mn^{III}_2(hmp)_6]$ SMM building blocks. Herein, we report synthesis and structure of

* Corresponding authors. Tel.: +7 496 52 21185; fax: +7 496 52 23507.
E-mail addresses: lkushch@icp.ac.ru, mila_g55@mail.ru (L.A. Kushch), yagubski@icp.ac.ru (E.B. Yagubskii).

1. Its magnetic properties as well as effect of irradiation on its optical properties are also analyzed.

2. Material and methods

The solvents and reagents were purchased from commercial sources and used as received. $[Mn_4(hmp)_6(NO_3)_2(H_2O)_2](ClO_4)_2\cdot4H_2O$ was prepared following a literature procedure [8]. $(PPh_4)_2[FeNO(CN)_5]$ was synthesized by metathesis in water using $Na_2[FeNO(CN)_5]$ and PPh_4Cl.

3. Experimental

3.1. Synthesis of $\{[Mn_4(hmp)_6(NO_3)_2FeNO(CN)_5]\cdot4CH_3CN\}_n$ (**1**) and preparation of its single crystals

At ambient temperature, an acetonitrile solution (10 mL) of $(PPh_4)_2[FeNO(CN)_5]$ (0.062 g, 0.07 mmol) was added dropwise under stirring to an acetonitrile solution (10 mL) of $[Mn_4(hmp)_6(NO_3)_2(H_2O)_2](ClO_4)_2\cdot4H_2O$ (0.09 g, 0.07 mmol). The resulting precipitate was collected by filtration, washed with acetonitrile and dried in vacuum to give the crimson polycrystalline powder of **1**. Yield: 0.062 g (68%). Elemental analysis indicates the loss of the solvent (CH_3CN) molecules. *Anal.* Calc. for $[Mn_4(hmp)_6(NO_3)_2FeNO(CN)_5]$: C, 40.75; H, 3.00; N, 16.22. Found: C, 40.50; H, 2.97; N, 16.12%. Characteristic IR data (cm^{-1}): $\nu(CN)$ 2133 (terminal), 2167 (bridge); $\nu(NO)$ 1893; $\nu(CN)$ 1604 (imine). Complex **1** is insoluble in common organic solvents. Single crystals suitable for an X-ray analysis were obtained by slow diffusion of starting reagents into clear solvent (CH_3CN) for one month. The crystals of **1** are highly sensitive to solvent loss; they are maintained in mother liquid to prevent solvent loss.

3.2. Physical measurements

Elemental analysis for C, H, and N were performed on a vario MICRO cube analyzing device. Infrared spectra (4000–500 cm^{-1}) were recorded using Varian 3100 FTIR Excalibur Series spectrometer. The photochromic properties of **1** were studied using Nicolet 5700 FTIR equipped with a variable-temperature (85–300 K) cryostat. The fine powder of **1** was mixed with KBr and pressed to a pellet. The KBr pellet was mounted on a copper cold finger using silver paste for good thermal contact. The sample was cooled to 85 K in cryostat. The presence of two KBr windows in cryostat allowed the irradiation of the sample with laser light (442 nm) and absorption measurement down to 390 cm^{-1}.

The DC magnetic susceptibility of powder sample **1** was measured by a Quantum Design MPMS-5 SQUID magnetometer in the temperature range between 1.84 and 300 K at the magnetic field 0.2 T. The experimental data were corrected for the sample holder and for the diamagnetic contribution calculated from Pascal constants. Effective magnetic moment was calculated using the equation $\mu_{eff} = 2.828\,(\chi_M \times T)^{1/2}$. Ac magnetic susceptibility measurements were performed on a PPMS magnetometer (Quantum Design) at various frequencies from 33 to 10,000 Hz with an ac field of 4 Oe and no dc field applied.
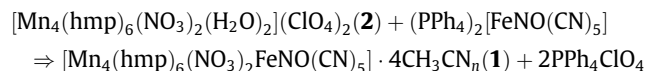
3.3. X-ray structural determination

A single-crystal X-ray diffraction study was carried out using an Oxford Diffraction Gemini-R diffractometer equipped with a two-dimensional Ruby CCD detector (red needle, $0.1 \times 0.03 \times 0.02$ mm³, λ(Mo Kα) = 0.71073 Å, graphite monochromator, ω-scans, range Θ = 2.77°–25.64°] and a low temperature Oxford Instruments Cryojet device at 150(1) K. CRYSALIS software [9] was used for cell refinement, data collection and data reduction with empirical absorption correction of experimental intensities (SCALE3ABSPACK program). The structure was solved by a direct method followed by Fourier syntheses and refined by a full-matrix least-squares method in an anisotropic approximation for all non-hydrogen atoms, with the SHELX-97 programs [10]. The positions of the H-atoms were calculated geometrically. Crystallographic data are summarized in Table 1.

4. Results and discussion

The heteropentametallic chain cluster $\{[Mn_4(hmp)_6(NO_3)_2Fe-NO(CN)_5]\cdot4CH_3CN\}_n$ (**1**) is a product of replacement of terminal H_2O ligands in the starting SMM (**2**) for bridging $FeNO(CN)_5$ ligands:

$$[Mn_4(hmp)_6(NO_3)_2(H_2O)_2](ClO_4)_2(\mathbf{2}) + (PPh_4)_2[FeNO(CN)_5]$$
$$\Rightarrow [Mn_4(hmp)_6(NO_3)_2FeNO(CN)_5]\cdot 4CH_3CN_n(\mathbf{1}) + 2PPh_4ClO_4$$

Compound **1** crystallizes in the triclinic space group $P\bar{1}$. Its structure is built from one-dimensional chains, wherein each chain is composed of alternating $[Mn_4(hmp)_6(NO_3)_2]^{2+}$ and $[FeNO(CN)_5]^{2-}$ units, Fig. 1. Nitroprusside anion, acting as a bidentate ligand via its two cyanide ligands, connects the Mn^{II} ions of $[Mn_4(hmp)_6(NO_3)_2]^{2+}$ clusters. The $[Mn_4]$ moiety has a typical double-cuboidal core containing two inner Mn^{III} ions (Mn2 and Mn2′) and two outer Mn^{II} ions (Mn1 and Mn1′), Fig. 2 [6,8,11]. The Mn^{II} ions are heptacoordinated, forming a slightly distorted pentagonal-bipyramidal coordination geometry, in which the five equatorial positions are occupied by NO_4 units (from the hmp⁻ ligands and NO_3 groups) and two axial ones coordinated by N atom of cyanide group and O atom of hydroxyl group with the interatomic Mn–N/O distances ranged from 2.187–2.360 Å, Table 2 (Mn–O distances are equal to 2.185, 2.201, 2.275 Å in the starting $[Mn_4(hmp)_6(NO_3)_2(H_2O)_2](ClO_4)_2\cdot4H_2O$ (**2**) cluster [8]). The internal Mn^{III} ions are hexacoordinated and present the Jahn–Teller elongation typical of a 3+ oxidation state. The interatomic distances for axial positions Mn2–O1 and Mn2–N2 are much longer (2.245 and 2.199 Å) with respect to 1.867 to 2.040 Å for equatorial ones (2.277 and 2.195 Å with respect to 1.860, 1.881 Å in **2**). The angle N2–Mn2–O1 is 160.79° (159.24° in **2**). The Jahn-Teller elongation axes in the crystal **1** are strictly parallel to each other in $[Mn_4]$ because of the presence of the inversion center at the midpoint of the core and they also parallel in the entire crystal (by crystal symmetry). The $Mn^{III}\cdots Mn^{III}$ separation in $[Mn_4]$ fragment is 3.200 Å (3.253 Å in **2**), and $Mn^{III}\cdots Mn^{II}$ 3.280 and 3.343 Å (3.271 and 3.364 Å in **2**). Structural analysis shows that the distances and the angles into $[Mn_4]$

Table 1
Crystal Data and structure refinement for **1**.

Compound	**1**
Formula	$C_{49}H_{48}FeMn_4N_{18}O_{13}$
Crystal system	triclinic
Space group	$P\bar{1}$
a (Å)	10.969(2)
b (Å)	11.726(2)
c (Å)	12.808(2)
α (°)	116.10(2)
β (°)	93.47(1)
γ (°)	97.83(1)
V (Å³)	1452.2(4)
Z	1
Reflection N (meas./uniq.)	14564/4624
Refinement parameters	387
Goodness of-fit-on (GOF) F^2	0.943
R_1 ($I > 2\sigma(I)$)*	0.075

* $R_1(F) = \Sigma||F_o| - |F_c||/\Sigma|F_o|$ for observed data.